

Organic Nanofibers from PPTPP

Frank Balzer¹, Manuela Schiek¹, Arne Lützeu² and Horst-Günter Rubahn¹

¹ Syddansk Universitet, Mads Clausen Institute, NanoSYD, Alsion 2, DK-6400 Sønderborg, Denmark
E-mail: fbalzer@mci.sdu.dk

² University of Bonn, Kekulé-Institute of Organic Chemistry and Biochemistry, Gerhard-Domagk-Str. 1, D-53121 Bonn, Germany

Abstract. The growth of 2,5-Di-4-biphenyl-thiophene (PPTPP) on the dielectric substrates NaCl, KCl, KAP, muscovite mica, and phlogopite mica is investigated by atomic force microscopy (AFM) and fluorescence microscopy. In all cases fibers are formed with several ten nanometers height and several hundred nanometers width, respectively. Only for PPTPP on muscovite mica the fibers are mutually parallel aligned along a single substrate direction, i.e. along muscovite $\langle 110 \rangle$. This uniaxial growth is explained by an electrostatic interaction between the molecules and surface electric fields in combination with epitaxy. The various growth directions on other substrates are dictated by epitaxy alone.

1. Introduction

Nanofibers from organic conjugated molecules such as bare and functionalized *para*-phenylenes [1,2], α -thiophenes [3], phenylene-thiophene co-oligomers [4,5], or coumarin derivatives [6] have a high application potential in future optoelectronic devices [7]. Waveguiding [8–10], tunable light emission [11], gain narrowing and lasing [12–14], as well as frequency doubling [15,16] have already been observed. In the past the growth of the blue-light emitting *para*-hexaphenylene (*p*-6P) molecules on muscovite mica and on KCl has been investigated in detail [17–20]. For *p*-6P on muscovite mutually parallel aligned needles along a single $\langle 110 \rangle$ substrate direction have been observed, their growth being steered by the anisotropic electric surface fields [21]. This $\langle 110 \rangle$ direction corresponds to the direction of grooves on the muscovite surface, which alternate by 120° in between consecutive cleavage planes. This direction is denoted as $\langle 110 \rangle_g$, the non-grooved one as $\langle 110 \rangle_{ng}$. The long molecule axis is oriented at $\pm 76^\circ$ with respect to muscovite $\langle 110 \rangle_g$, resulting in a single energetically favorable needle orientation. Low energy electron diffraction (LEED) and thermal desorption spectroscopy (TDS) have shown, that the first growth step is the formation of a wetting layer from lying molecules. Then clusters grow, and finally these clusters aggregate into needles. On KCl no such wetting layer and almost no clusters have been detected [22]. Needles grow along the two $\langle 110 \rangle$ substrate directions simultaneously [23].

For the investigated rod-like molecules so far the possible needle directions on muscovite depend on the epitaxial orientation of the molecules on the substrate, and on the packing of these molecules within a needle [24]. Therefore *para*-functionalized *para*-phenylenes show a very similar growth behavior compared to *p*-6P. The α -thiophenes quaterthiophene and sexithiophene, however, align with their long molecular axes along the two muscovite high symmetry directions without

a groove, i.e. along $\langle 110 \rangle_{\text{ng}}$, and $[100]$, and therefore three needle orientations are accomplished simultaneously. That way fortunate optical properties of an uniaxially aligned needle film such as polarized light absorption and emission are lost. To preserve some of the phenylene growth properties but, e.g., change the emission color substantially we therefore have investigated the growth of a thiophene phenylene co-oligomer: 2,5-Di-4-biphenyl-thiophene (PPTPP), Fig. 1. Here we show first results for growth experiments on different substrate surfaces under similar growth conditions, i.e. similar substrate temperatures T_s , deposition rates, and nominal film thicknesses.

2. Experimental Methods

2,5-Di-4-biphenyl-thiophene has been synthesized in a two-fold Suzuki cross-coupling reaction from commercially available 2,5-dibromo-thiophene and 4-biphenyl boronic acid, using 5 mol% tetrakis(triphenylphosphino)palladium as catalyst together with cesium fluoride as base in dry tetrahydrofuran. The desired product has been obtained in yields of 80% after refluxing for 50 h. The final product precipitated from the reaction mixture and was washed with water and organic solvents repeatedly for purification. By outgassing in vacuo residual organic solvents are removed to give the desired compounds in high purity. Note that PPTPP has been synthesized previously using very similar approaches [25,26].

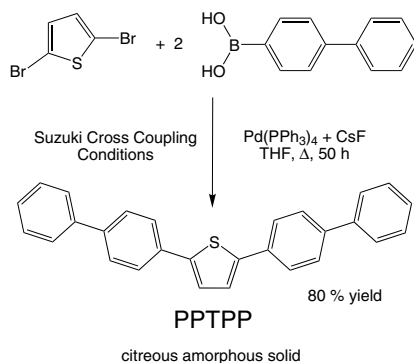


Fig. 1. Schematics of the synthesis of 2,5-Di-4-biphenyl-thiophene (PPTPP).

As substrate materials five different single crystals have been chosen: potassium chloride (KCl), sodium chloride (NaCl), potassium acid phthalate (KAP) [27], muscovite mica [28], and phlogopite mica. All are cleaved in air and are transferred immediately into a high vacuum system (base pressure 2×10^{-8} mbar). Either right away or after annealing a clear low energy electron diffraction (MCP-LEED, Omicron) pattern is observed for each of them. Organic molecules are deposited from an effusion cell. The nominal deposited film thickness is estimated by a water-cooled quartz microbalance located next to the substrate.

After deposition the samples are characterized in situ by LEED, ex situ by atomic force microscopy (AFM, JPK NanoWizard) and fluorescence microscopy (excitation wavelength $\lambda_{\text{exc}} = 365$ nm from a high-pressure mercury lamp).

3. Results and Discussion

Figure 2 shows $150 \times 150 \mu\text{m}^2$ fluorescence microscope images of typical samples deposited at $T_s = 350$ K – 380 K with a deposition rate of $0.1 \text{ \AA/s} - 0.2 \text{ \AA/s}$ and nominal thicknesses up to 5 nm. On all of those substrates needle-like structures from PPTPP form. All emit blue-green light after normal incidence UV irradiation. The emitted fluorescence from the needles is strongly polarized, the polarization vector being oriented perpendicular to the local needle direction. Similar to the case of, e.g., *p*-6P [21,29,30] this points to fibers made from lying organic molecules, the long molecular axis being perpendicular to the long needle axis. In addition for all substrates except for muscovite mica a green light emitting background is visible. This can be clearly seen in Fig. 2(c), where the border between the bare substrate and the deposition area is imaged. Typical fluorescence spectra are presented in Fig. 3. A well resolved vibronic progression is visible between 400 nm

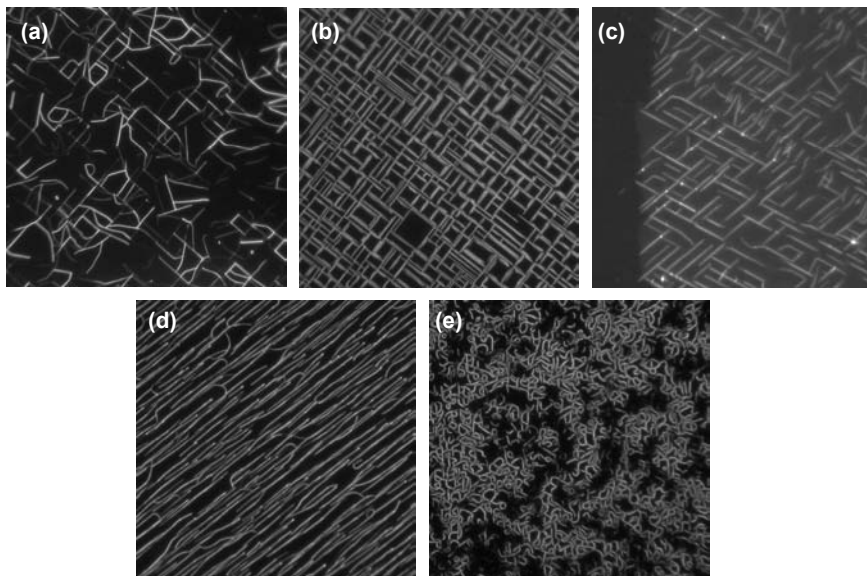


Fig. 2. Fluorescence microscope images, $150 \times 150 \mu\text{m}^2$, of PPTPP on (a) NaCl, (b) KCl, (c) KAP, (d) muscovite mica, and (e) phlogopite mica. The nominal thickness of all samples is between 2 nm and 5 nm, the surface temperature during deposition varies between $T_s = 350$ K – 380 K.

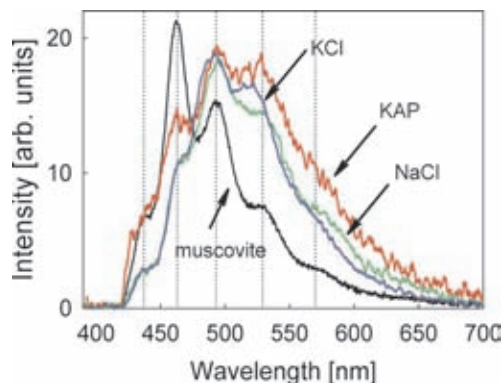


Fig. 3. Unpolarized measured fluorescence spectra of PPTPP needle films on different substrates after excitation with unpolarized $\lambda_{\text{exc}} = 365$ nm light under normal incidence. The dotted vertical lines mark the peak positions at 437 nm, 463 nm, 493 nm, 529 nm, and 570 nm.

and 600 nm with an energy spacing of approximately 1300 cm^{-1} , being most prominent in the case of muscovite and phlogopite mica. Slightly different colors in the microscopy images stem from different relative intensities of the excitonic transitions. The reason for the distribution of intensity between the fluorescence peaks is still unknown, but might be related to different molecule–molecule interactions for the molecules forming the patches of upright molecules, see below, and for molecules forming needles [31].

Although needle-like structures are formed in all five cases, the realized needle directions depend very much on the substrate. On NaCl, KCl, and KAP two needle directions evolve, with different angles in between. On NaCl and KCl the angle is 90° , and the needles grow along the two substrate $\langle 110 \rangle$ directions simultaneously. On KAP the angle is 68° , corresponding to the angle between the two KAP $\langle 101 \rangle$ directions [32]. On muscovite mica all of the needles grow along a single $\langle 110 \rangle$ direction, with altogether two orientational domains being present on the whole sample. On phlogopite mica three different growth directions exist, most pronounced at the very early growth stages and for deposition at room temperature. For larger coverages and higher substrate temperatures the needles tend to curl and to form rings. To a lesser extent this curling is also observed for PPTPP on NaCl and muscovite, Figs. 2(a) and (d), the tendency increasing with the overall needle length.

Corresponding AFM images (see Fig. 4) provide widths and heights of the needles, but also show in more detail the greenish background from Fig. 3. This background results from patches of one or two multiples of approximately 2.2 nm height, suggesting that they are formed from upright molecules [25]. This background appears for all substrates except for muscovite mica, where clusters appear instead. These clusters are also found on phlogopite mica. They do not exist directly besides the needles (denuded zones).

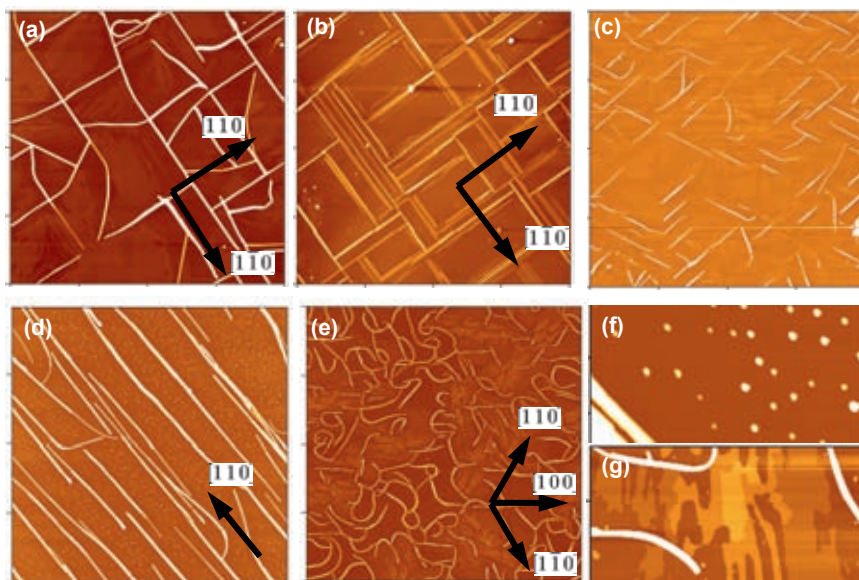


Fig. 4. Atomic force microscope images, $40 \times 40 \mu\text{m}^2$, of PPTP on (a) NaCl, (b) KCl, (c) KAP, (d) muscovite mica, and (e) phlogopite mica, corresponding to the fluorescence microscope images from Fig. 2. The height scales are (a) – (c) 100 nm, and (d) – (e) 50 nm. Arrows emphasize substrate directions. In the $5 \times 2.5 \mu\text{m}^2$ AFM images for muscovite (f) and phlogopite (g) the clusters from lying molecules as well as layers from upright ones are clearly visible.

4. Conclusions and Outlook

Obviously the growth directions of the needles depend strongly on the crystal structure of the underlying substrates. The symmetry of the substrate is retained in the needles' growth directions. Similar to the case of *p*-6P we attribute this observation to an epitaxial relationship of the organic molecules with the corresponding substrate. On NaCl and on phlogopite the alignment is not as perfect as for KCl and muscovite mica, respectively.

The uniaxial growth on muscovite mica is explained by an electrostatic interaction between the molecules and surface electric fields in combination with epitaxy. Epitaxy leads to an alignment of the molecules along muscovite high symmetry directions, whereas the electric fields choose the energetically most favorable of the three possible growth directions: needles grow along $\langle 110 \rangle_g$. Muscovite and phlogopite mica exhibit almost identical lattice constants and surface compositions, but differ in that phlogopite is a trioctahedral mica, whereas muscovite is a dioctahedral one. This leads to the already describe grooves along a single $\langle 110 \rangle$ direction on muscovite, which are missing on phlogopite [33]. Therefore on phlogopite three simultaneous needle directions exist, on muscovite only one.

Not only the realized needle directions, but also the growth mechanism is similar to the case of *p*-6P. The observed clusters on muscovite and phlogopite are remnants from the initial growth stage. Only when the cluster number density reaches a critical value, needles start growing, mainly by agglomeration of the clusters. A LEED pattern from a wetting layer of lying molecules is observed for the case of muscovite mica. For all other cases no such diffraction pattern has been detected.

As a conclusion the growth mechanism of PPTPP and the realized needle directions on the different substrates are similar to that of *p*-6P. Understanding such basic growth principles allows one to predict qualitatively nanowire surface growth from other conjugated molecules and thus allows for a sophisticated design of new devices. Adding, for example, another thiophene ring next to the existing one to form 5,5'-Di-4-biphenyl-2,2'-bithiophene (PPTPP) does not alter the basic growth mode, but changes the epitaxial alignment on muscovite. From that two simultaneous needle directions on muscovite are predicted and are actually observed [24].

Acknowledgements. We are grateful to the Danish research agencies FNU and FTP as well as the Danish Advanced Technologies Trust for supporting this work by various grants. MS and AL thank the German research foundation DFG for financial support.

References

- 1 F. Balzer and H.-G. Rubahn, *Adv. Funct. Mater.*, **15**, 17, 2005.
- 2 M. Schiek, F. Balzer, K. Al-Shamery, A. Lützeu, and H.-G. Rubahn, *Soft Matter*, **4**, 277, 2008.
- 3 F. Balzer, L. Kankate, H. Niehus, and H.-G. Rubahn, *Proc. SPIE*, **5724**, 285, 2005.
- 4 H. Yanagi, T. Morikawa, S. Hotta, and K. Yase, *Adv. Mater.* **13**, 313, 2001.
- 5 F. Balzer, M. Schiek, A. Lützeu, K. Al-Shamery, and H.-G. Rubahn, *Proc. SPIE* **6470**, 647006, 2007.
- 6 M. Mille, J.-F. Lamere, F. Rodrigues, and S. Fery-Forgues, *Langmuir* **24**, 2671, 2008.
- 7 K. Al-Shamery, H.-G. Rubahn, and H. Sitter, editors. *Organic Nanostructures for Next Generation Devices*, Vol. 101 of *Springer Series in Materials Science*, Berlin 2008.
- 8 K. Takazawa, *Chem. Phys. Lett.* **452**, 168, 2008.
- 9 H. Yanagi and T. Morikawa, *Appl. Phys. Lett.* **75**, 187, 1999.
- 10 F. Balzer, V.G. Bordo, A.C. Simonsen, and H.-G. Rubahn, *Phys. Rev. B* **67**, 115408, 2003.
- 11 Y.S. Zhao, H. Fu, F. Hu, A. Peng, W. Yang, and J. Yao, *Adv. Mater.* **20**, 79, 2008.
- 12 F. Quochi, F. Cordella, A. Mura, G. Bongiovanni, F. Balzer, and H.-G. Rubahn, *J. Phys. Chem. B* **109**, 21690, 2005.
- 13 F. Quochi, F. Cordella, R. Orru, J.E. Communal, P. Verzeroli, A. Mura, G. Bongiovanni, A. Andreev, H. Sitter, and N.S. Sariciftci, *Appl. Phys. Lett.* **84**, 4454, 2004.
- 14 H. Yanagi, T. Ohara, and T. Morikawa, *Adv. Mater.* **13**, 1452, 2001.
- 15 F. Balzer, J. Brewer, J. Kjølstrup-Hansen, M. Madsen, M. Schiek, K. Al-Shamery, A. Lützeu, and H.-G. Rubahn, *Proc. SPIE* **6779**, 67790I, 2007.

- 16 J. Brewer, M. Schiek, A. Lützeu, K. Al-Shamery, and H.-G. Rubahn, *Nano Lett.* **6**, 2656, 2006.
- 17 L. Kankate, F. Balzer, H. Niehus, and H.-G. Rubahn, *J. Chem. Phys.* **128**, 084709, 2008.
- 18 A. Andreev, T. Haber, D.-M. Smilgies, R. Resel, H. Sitter, N.S. Sariciftci, and L. Valek, *J. Cryst. Growth* **275**, e2037, 2005.
- 19 A.Y. Andreev, C. Teichert, G. Hlawacek, H. Hoppe, R. Resel, D.-M. Smilgies, H. Sitter, and N.S. Sariciftci, *Org. Electron.* **5**, 23, 2004.
- 20 P. Frank, G. Hlawacek, O. Lengyel, A. Satka, C. Teichert, R. Resel, and A. Winkler, *Surf. Sci.* **601**, 2152, 2007.
- 21 F. Balzer and H.-G. Rubahn, *Appl. Phys. Lett.* **79**, 3860, 2001.
- 22 P. Frank, G. Hernandez-Sosa, H. Sitter, and A. Winkler, *Thin Solid Films* **516**, 2939, 2008.
- 23 T. Mikami and H. Yanagi, *Appl. Phys. Lett.* **73**, 563, 1998.
- 24 F. Balzer, M. Schiek, K. Al-Shamery, A. Lützeu, and H.-G. Rubahn, *J. Vac. Sci. Technol. B* **26**, 2008. In print.
- 25 T.J. Dingemans, N.S. Murthy, and E.T. Samulski, *J. Phys. Chem. B* **105**, 8845, 2001.
- 26 S. Hotta, H. Kimura, S.A. Lee, and T. Tamaki, *J. Heterocycl. Chem.* **37**, 281, 2000.
- 27 M. Campione, A. Sassella, M. Moret, A. Papagni, S. Trabattoni, R. Resel, O. Lengyel, V. Marcon, and G. Raos, *J. Am. Chem. Soc.* **128**, 13378, 2006.
- 28 E.W. Radoslovich, *Acta Cryst.* **13**, 919, 1960.
- 29 A. Andreev, G. Matt, C.J. Brabec, H. Sitter, D. Badt, H. Seyringer, and N.S. Sariciftci, *Adv. Mater.* **12**, 629, 2000.
- 30 A. Niko, E. Zojer, F. Meghdadi, C. Ambrosch-Draxl, and G. Leising, *Synth. Met.* **101**, 662, 1999.
- 31 E. Da Como, M.A. Loi, M. Murgia, R. Zamboni, and M. Muccini, *J. Am. Chem. Soc.* **128**, 4277, 2006.
- 32 A.V. Alex and J. Philip, *J. Appl. Phys.* **88**, 2349, 2000.
- 33 Y. Kuwahara, *Phys. Chem. Miner.* **28**, 1, 2001.

Interface Controlled Organic Thin Films

Rubahn, H.-G.; Sitter, H.; Horowitz, G.; Al-Shamery, K.
(Eds.)

2009, XII, 230 p. 122 illus., 8 illus. in color., Hardcover

ISBN: 978-3-540-95929-8